ImmunoHorizons

RESEARCH ARTICLE | OCTOBER 01 2021

Transcriptomic Analysis of Healthy and Atopic Dermatitis Samples Reveals the Role of IL-37 in Human Skin

Jiajun Zhou; ... et. al

Immunohorizons (2021) 5 (10): 830–843.
https://doi.org/10.4049/immunohorizons.2100055

Transcriptomic Analysis of Healthy and Atopic Dermatitis Samples Reveals the Role of IL-37 in Human Skin

Jiajun Zhou,* David C. Gemperline,* Matthew J. Turner,[†,‡] Jonathan Oldach,[§] Jennifer Molignano,[§] Jonathan T. Sims,* and Keith R. Stayrook*,[1]

*Lilly Research Laboratory, Eli Lilly and Company, Indianapolis, IN; [†]School of Medicine, Indiana University, Indianapolis, IN; [‡]Richard L. Roudebush Veterans Affairs Medical Center, Indianapolis, IN; and [§]MatTek Life Sciences, Ashland, MA

ABSTRACT

Atopic dermatitis (AD) is a chronic inflammatory skin disease that affects up to one in five children and millions of adults in developed countries. Clinically, AD skin lesions manifest as subacute and/or chronic lichenified eczematous plaques, which are often intensely pruritic and prone to secondary bacterial and viral infections. Despite the emergence of novel therapeutic agents, treatment options and outcomes for AD remain suboptimal. An improved understanding of AD pathogenesis may help improve patient outcomes. Dysregulated T_h2-polarized skin inflammation and impaired skin barrier function interact to drive AD pathogenesis; however, much remains to be understood about the molecular mechanisms underlying this interplay. The current study used published clinical trial datasets to define a skin-related AD gene signature. This meta-analysis revealed significant reductions in *IL1F7* transcripts (encodes IL-37) in AD patient samples. Reduced *IL1F7* correlated with lower transcripts for key skin barrier function genes in the epidermal differentiation complex. Immunohistochemical analysis of normal (healthy) human skin specimens and an in vitro three-dimensional human skin model localized IL-37 protein to the epidermis. In comparison with normal human skin, IL-37 levels were decreased in AD patient skin. Addition of T_h2 cytokines to the aforementioned in vitro three-dimensional skin model recapitulates key aspects of AD skin and was sufficient to reduce epidermal IL-37 levels. Image analysis also indicated close relationship between epidermal IL-37 and skin epidermal differentiation complex proteins. These findings suggest IL-37 is intimately linked to normal keratinocyte differentiation and barrier function and implicates IL-37 as a potential biomarker and therapeutic target for AD. *ImmunoHorizons*, 2021, 5: 830–843.

INTRODUCTION

Atopic dermatitis (AD) is a classified as chronic inflammatory skin disorder that affects around 15–20% of people in developed countries. AD develops during early childhood with the characteristic of recurrent eczematous lesion with strong itch and discomfort. Around 10–30% of patients will continue to have various symptoms progressing into adulthood (1). AD is a heterogenous disease with a wide spectrum of clinical features (i.e., minimal flexural eczema to erythroderma [affecting more than 90% of the body surface] to eczema limited to the hands) (2). Pruritus (itch), associated insomnia, secondary skin infections, and social stigmata can impair quality of life in AD (3, 4).

Mechanistic studies have shown that T_h2 cells and epidermal disruption contribute to the development of AD (5). Immunological alterations in AD patients include disproportion activation of T_h2 lymphocytes and consequent release of T_h2 cytokines (IL-4, IL-13, IL-5, and IL-31), which in turn activates other immune cells (e.g., macrophages and B cells) to promote inflammatory cascades implicated in pathogenesis (6). Impaired skin barrier

Received for publication June 15, 2021. Accepted for publication September 24, 2021.

Address correspondence and reprint requests to: Dr. Jonathan T. Sims, Lilly Research Laboratory, Eli Lilly and Company, Lilly Corporate Center, 893 S. Delaware Street, Indianapolis, IN 46225. E-mail address: sims_jonathan_thomas@lilly.com

ORCIDs: 0000-0001-5877-4306 (J.O.); 0000-0001-8599-2157 (J.T.S.).

[1]Current address: Asteroid Therapeutics, Indianapolis, IN.

Abbreviations used in this article: AD, atopic dermatitis; 3D, three-dimensional; EDC, epidermal differentiation complex; FDR, false discovery rate; FLG, Filaggrin; IHC, immunohistochemistry; IVL, involucrin; LOR, loricrin; LSD, least significant difference; rhIL-37, human rIL-37; RT, room temperature.

The online version of this article contains supplemental material.

https://doi.org/10.4049/immunohorizons.2100055

ImmunoHorizons is published by The American Association of Immunologists, Inc.

function is the other hallmark of AD and can arise from somatic mutations, a result from impaired keratinocyte differentiation in response to allergic skin inflammation (7). Only 40% of AD patients harbor *Filaggrin* (*FLG*) mutation, the rest of patients do not carry *FLG* mutations but often exhibit reduced levels of FLG protein expression in the epidermis owing to the ability of T_h2 cytokines like IL-4 to impair keratinocyte differentiation and, thus, *FLG* expression (8). Autosomal semidominant *FLG* mutations leading to suboptimal levels of FLG protein impair skin barrier function and are found in a significant proportion (but a minority) of patients with AD (9). Impaired FLG production and other associated impairments in skin barrier function in AD alter structural and physiochemical properties of the stratum corneum and tight junctions in the epidermis, resulting in a compromised skin barrier. A compromised skin barrier leads to excessive water loss from the skin and provides a means for microbial pathogens and their component parts to breach the skin barrier, leading to infection and/or promotion of allergic skin inflammation (10). In addition to *FLG*, T_h2 and other cytokines can impair the ability of keratinocytes to differentiate and produce other skin structural proteins such as loricrin (LOR) and involucrin (IVL), further disrupting the skin barrier in AD patients (11, 12).

Structural proteins like FLG and IVL are critical for epidermal homeostasis of the skin. FLG plays a fundamental role in terminal epidermal differentiation and for the implication in common dermatological diseases (13). Similar to FLG, IVL is important during the early steps of skin barrier formation, establishing that the outermost protein layer for the covalent attachment of ceramide lipids human LOR is the most abundant component of the epidermal skin barrier. Mutation of the *FLG* gene, change in the skin microenvironment, or external factors all have been demonstrated as key contributors to the decrease of FLG expression. FLG deficit has a major impact on the epidermal barrier, leading to the decrease of organization of the keratin filaments of the cytoskeleton and structure of the cornified envelope (14–16).

IL-37

IL-37 (*IL-1F7*) is a recently discovered member of the IL-1 cytokine family. Members of this cytokine family are important mediators of innate and adaptive immune responses. Recent studies demonstrate changes in IL-37 expression in cancers, chronic inflammatory diseases, and autoimmune disorders (17). There are five known isoforms of IL-37 (IL-37a, IL-37b, IL-37c, IL-37d, and IL-37e), with IL-37b and IL-37d encoding functional proteins (18). A variety of cell types of express IL-37, including NK cells, B cells, monocytes, epidermal keratinocytes, and other epithelial cells. IL-37b expression is the most prominent isoform in leukocytes and epithelial cells, including those in the skin as well as the respiratory and gastrointestinal tracts (17). Emerging evidence also shows IL-37 can be expressed at low levels in some human cells and tissues and be upregulated via TLR activation and by other inflammatory stimuli (19, 20).

In the current study, we conducted meta-analysis of published skin-related clinical trial transcriptomics datasets to understand the relationship between AD and skin barrier function. This analysis revealed IL-37 transcripts are significantly decreased in AD patient skin and identified a positive correlation between IL-37 transcripts and expression of epidermal differentiation complex (EDC) transcripts. The positive correlation of *IL-37* transcripts with skin structural genes (*FLG*, *FLG2*, and *IVL*) provides a possible link between IL-37 and skin barrier function. In addition, we observed colocalization of IL-37 and EDC proteins in, or in proximity to, the stratum. Compared with healthy human skin, immunostaining in AD patient skin revealed significant reductions in IL-37 protein. Similar reductions were observed in an in vitro three-dimensional (3D) skin model of AD. Overall, the current study is the first, to our knowledge, to highlight the coexpression of epidermal IL-37 and EDCs proteins and provides evidence that T_h2 cytokines might account for the observed reduction in IL-37 expression in AD skin specimens.

MATERIALS AND METHODS

Clinical skin sample collection

This study included skin and blood samples obtained from moderate-to-severe AD from two phase 2 clinical studies (AD-1: n = 10 from phase 2 study, including concomitant topical corticosteroid use [NCT02576938, first posted to ClinicalTrials.gov on October 15, 2015], and AD-2: n = 20 from phase 2 study of patients washed out from all systemic therapeutics at study entry [NCT03831191, first posted to ClinicalTrials.gov on February 5, 2019]). Additional skin samples (n = 10) were collected from patients with no topical medications applied to skin for a period of at least 1 wk before samples were collected through collaboration with Indiana University. All patients provided informed consent prior to sample collection. The collection of the patient skin biopsy was done under a Food and Drug Administration–approved clinical protocol. Two independent groups of healthy control subjects with no history of autoimmune disorders were included for evaluation of either skin (n = 10) or blood (n = 10) biomarkers.

Data collection and processing

Eight gene expression datasets (GSE107361, GSE32924, GSE36842, GSE5667 GPL96, GSE5667 GPL97, GSE60709, GSE75890, and PRJNA496323) of AD skin biopsies from Gene Expression Omnibus were obtained and analyzed. For each study, the sample phenotypes were defined by the corresponding original publications. The microarray probes were mapped in each dataset to Entrez Gene identifiers. If a probe matched more than one gene, the expression data for the probe were expanded to add one record for each mapped gene.

https://doi.org/10.4049/immunohorizons.2100055

Meta-analysis for differentially expressed genes

The effect size of each gene in each dataset as Hedge adjusted g accounted for small sample bias. In the case of multiple probes mapped, the effect size for each gene used the fixed-effect inverse-variance model. The study-specific effect sizes for each gene into a single meta-effect size used a linear combination of study-specific effect sizes for each gene into a single meta-effect size using a linear combination of study-specific effect sizes, f_i, in which each study-specific effect size was designated by the inverse of the variance in the corresponding study. After calculating the meta-effect size, significant genes using the Z statistic and corrected p values for multiple hypothesis were tested using Benjamini–Hochberg false discovery rate (FDR) correction (21). Fisher sum of logs methods was used for meta-analysis by combining p value. For each gene, the logarithm of the one-sided hypothesis tested p values across k studies and compared the result with a χ^2 distribution with $2k$ degree of freedom. This process allowed us to identify significant genes. Differentially expressed genes were selected based on the follow criteria: 1) absolute summary effect size >1.5, 2) FDR ≤5% across all datasets when combining effect size, 3) measured in all discovery datasets, and 4) when combining p value using Fisher test, FDR ≤5%.

Quantitative real-time PCR

The probes used in the studies were *FLG* (HS00856927_g1), *FLG2* (Hs00418578_m1), *LOR* (Hs01894962_s1), *IVL* (Hs00846307_s1), *IL-37* (IL-1-h7; Hs00367201_m1), and 18s (Hs99999901_s1). RNA was isolated using Qiagen RNeasy kits following the manufacturer's instructions. RNA concentrations were assessed using Nanodrop ND-8000 Scientific spectrophotometer (Thermo Fisher Scientific), and around 300 ng of RNA per sample was processed following the instruction of High-Capacity cDNA RT-PCR kit (4368814; Thermo Fisher Scientific) by Applied Biosystems for reverse transcription to obtain cDNA library. The cDNA was amplified using Applied Biosystems TaqMan Gene Expression Assays. All quantitative real-time PCR reactions were performed on an Applied Biosystems QuantStudio 7 Flex Real-Time PCR System. Human 18S rRNA (Applied Biosystems) was used as an internal control. Fold change in gene expression was calculated using the ΔΔCt method.

Human full thickness EpidermFT-400 3D In Vitro Skin Model by MatTek

An AD-like phenotype was induced in the EpidermFT-400 3D In Vitro Skin Model (EpidermFT) according to the manufacturer's recommended protocol (22). Briefly, human rIL-4 (30 ng/ml), IL-13 (30 ng/ml), and IL-31 (15 ng/ml) (PeproTech) were added to the culture media for a total of 3 d. Tissues cultured in media without the addition of IL-4, IL-13, and IL-31 served as a control (EpidermFT). To study the effect of IL-37 on the EpidermFT model, human rIL-37 (rhIL-37; R&D Systems) was added to the culture media with and without the addition of IL-4, IL-13, and IL-31. On day 3 following the addition of cytokines to induce the AD phenotype, EpidermFT tissues were bisected. RNA was isolated from one half of each tissue and subsequently used for quantitative RT-PCR. The remaining half of each EpidermFT tissue was fixed in 10% neutral buffered formalin, embedded in paraffin, and sectioned to prepare slides for immunohistochemistry (IHC).

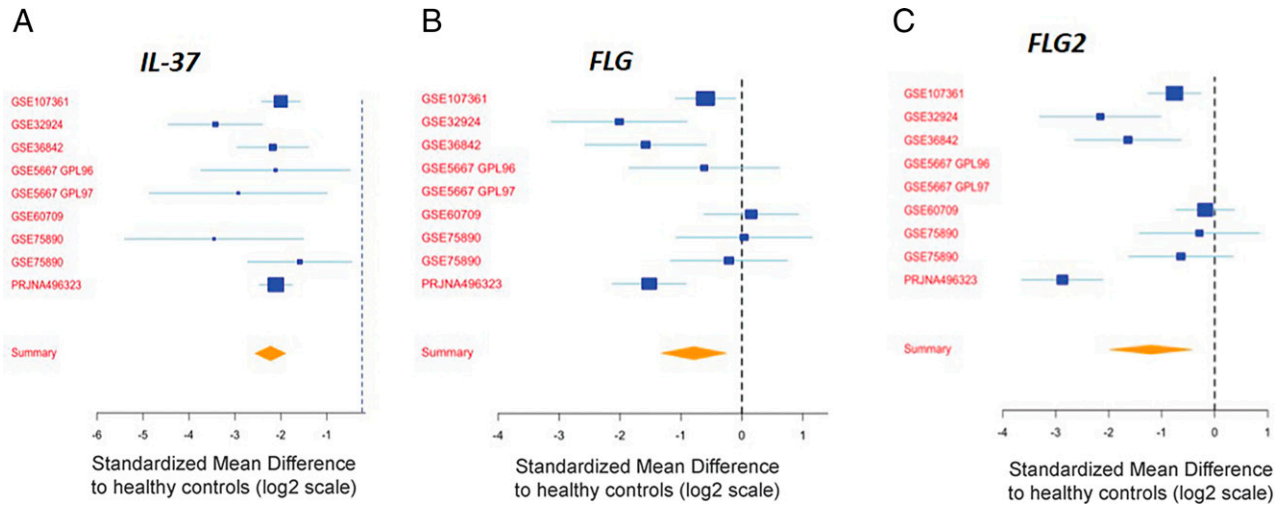

FIGURE 1. IL-37 and EDCs expression in skin RNA sequencing datasets.

Gene expression in AD clinical trials. (**A**–**C**) Gene expression in nine publicly available datasets. Expression of (A) *IL-37*, (B) *FLG*, and (C) *FLG2* in AD patients compared with healthy controls. The gene expression is normalized to healthy controls within respective datasets. The dotted line on the graph represented baseline expression of each gene.

Immunohistochemistry

Clinical biopsy samples (trial AD-1 and AD-2) were fixed in formalin, embedded in paraffin, and sectioned prior to performing IHC. The Abs used in the staining included slides prepared from clinical samples, and EpidermFT model tissue were deparaffinized and rehydrated in dH_2O for 15 min before initiating staining. To perform Ag retrieval, slides were incubated with freshly prepared 0.05% citraconic anhydride (pH 7.4) for 45 min at 98°C. Slides were cooled at room temperature (RT) for 20 min, then washed three times with dH_2O. Samples were blocked with 10% normal goat serum + 1% BSA in PBS for 1 h at RT. Primary Abs were diluted in 1% PBS in PBS + 0.1% Tween 20. EpidermFT tissue sections were probed for FLG (ab218395, 1 μg/ml; Abcam), IVL (ab53112, 10 μg/ml; Abcam), FLG2 (ab122011, 2 μg/ml; Abcam), and IL-37 (HPA054371, 1 μg/ml; Sigma-Aldrich) individually, whereas clinical samples were probed with IVL (ab181980, 1.36 μg/ml; Abcam), FLG (ab234406, 1 μg/ml; Abcam), and FLG2 (ab122011, 2 μg/ml; Abcam), all costained with IL-37 (60296-1-IG, 1.5 μg/ml; Thermo Fisher Scientific). Tissue sections were incubated with diluted primary Abs for 1 h at RT. Following incubation with primary Abs, the slides were washed twice with 5× TBST and once with 1× TBST for 5 min each. Diluted secondary Abs (Alexa Fluor 488 Goat Anti-mouse IgG Ab, A11001 [Thermo Fisher Scientific]; and Alexa Fluor 555 Goat Anti-rabbit IgG Ab, A21428, diluted 1:400 in 1% BSA in PBS + 0.1% Tween 20 [Thermo Fisher Scientific]) were then added to the tissue sections and incubated for 1 h at RT. Following incubation with secondary Abs, the slides were washed twice with 1× TBST for 5 min each. Slides were incubated with diluted DAPI (1:47,000) solution prepared in water for 10 min at RT then washed with 1× TBST twice. After washing, the tissue sections were covered with Immu-Mount mounting solution (Thermo Fisher Scientific), and coverslips were applied. All slides were imaged on the Olympus VS100 slide scanner using a 10× objective for the EpidermFT samples and a 20× objective for clinical trial samples.

Image analysis

All the immunofluorescence images were analyzed by HALO software developed by Indica Labs (version 3.0.311.201). For the clinical biopsy samples, images were uploaded onto the HALO software, and the images were visualized with DAPI (blue) for nuclear staining, FITC (green) for IL-37, and tetramethylrhodamine isothiocyanate (red) for FLG/FLG2/IVL. For the EpidermFT samples, blue color

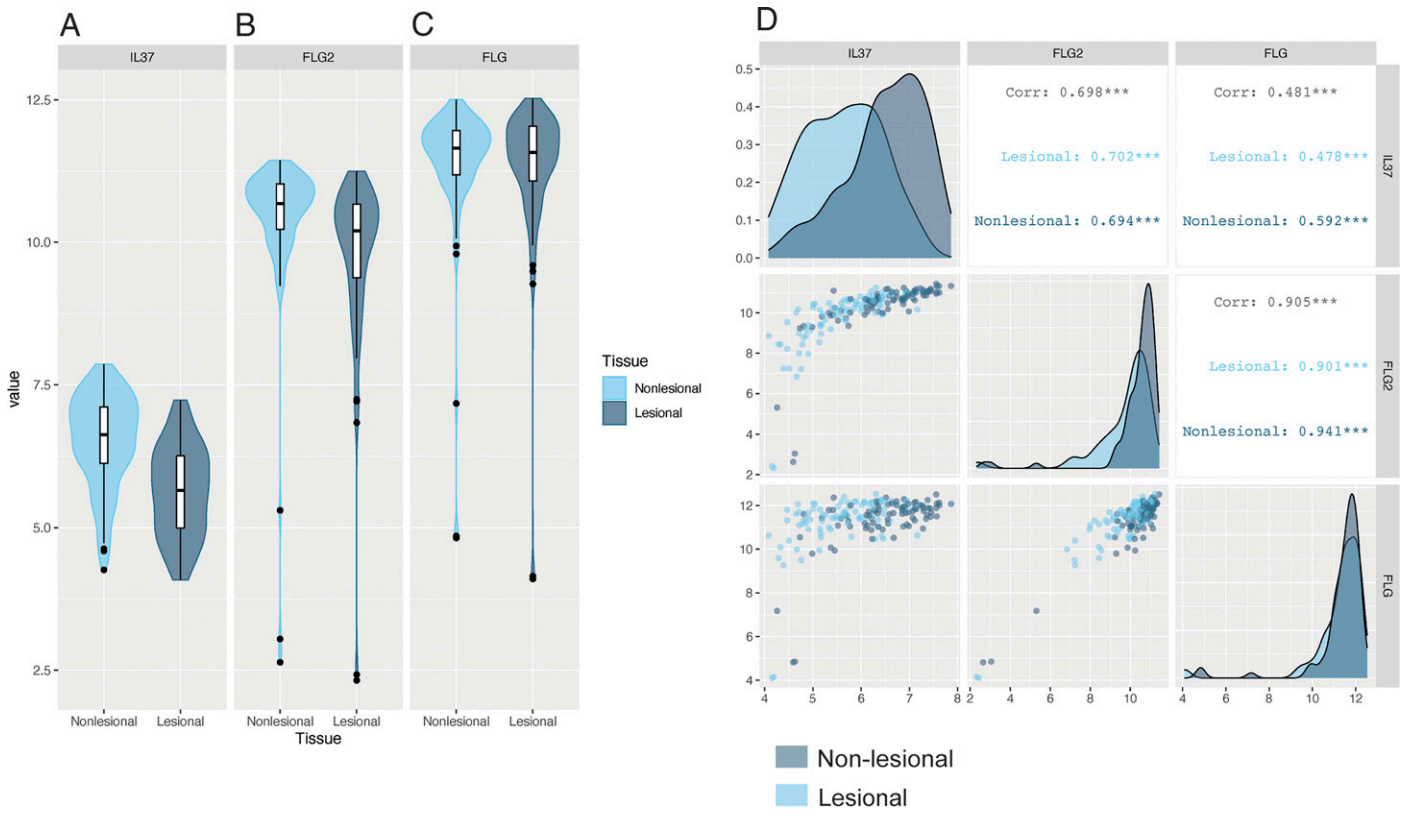

FIGURE 2. Gene expression in AD clinical trial.

Gene expression in moderate-to-severe AD patients from AD-1 clinical trials. Comparison of expression of (**A**) *IL-37*, (**B**) *FLG2*, and (**C**) *FLG* between nonlesional AD samples to lesional AD samples. (**D**) Correlation of *IL-37* expression with *FLG* and *FLG2* AD-1 trial. *$p < 0.05$ for nonlesional tissues to lesional tissues by unpaired *t* test.

https://doi.org/10.4049/immunohorizons.2100055

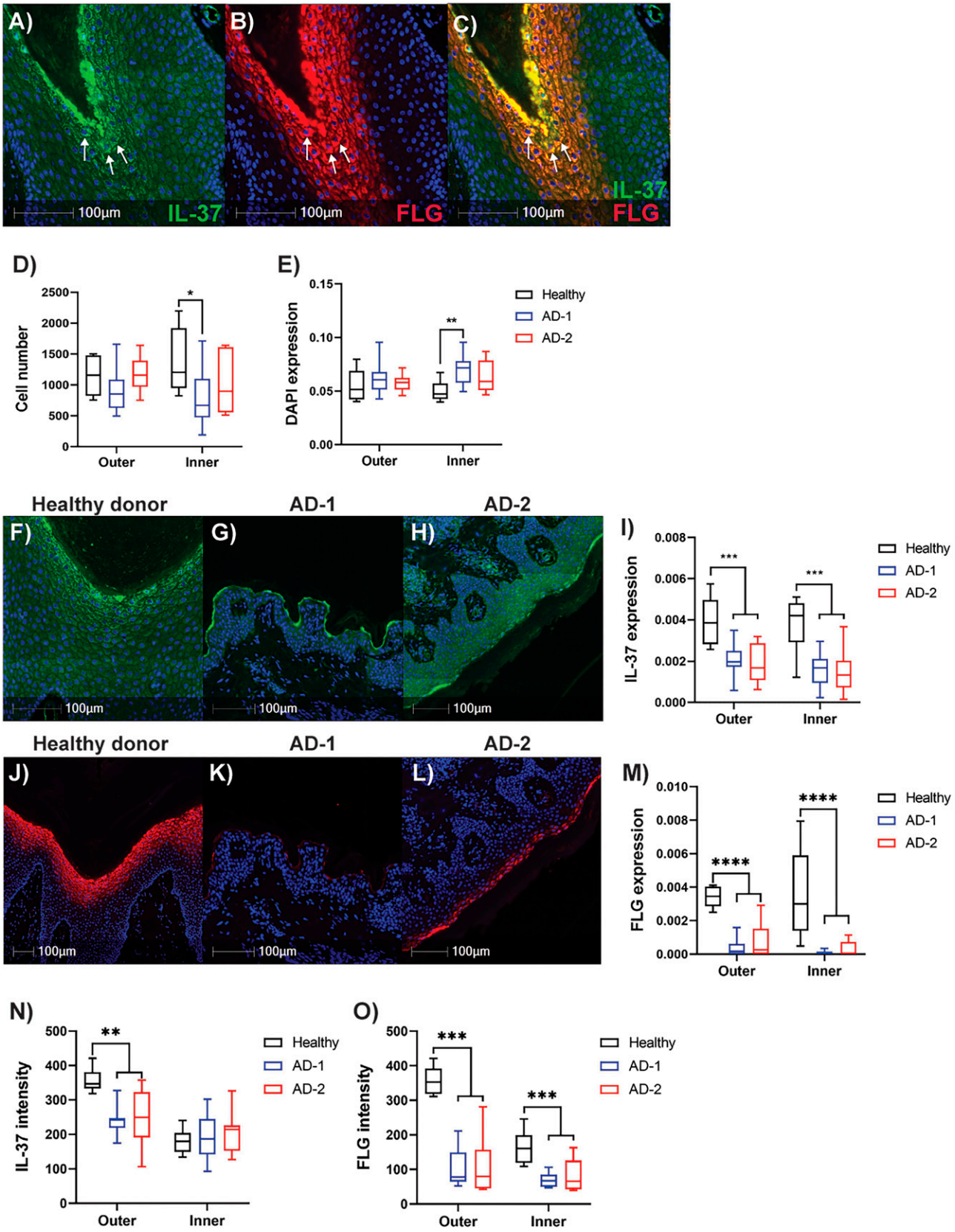

FIGURE 3. Immunofluorescent staining of FLG and IL-37 in healthy and AD skin biopsies.

Immunofluorescent staining of FLG (red) and IL-37 (green). The detail of the staining and image processes can be found in *Materials and Methods*. The nuclear staining (DAPI) is in blue. Immunostaining against (**A**) IL-37, (**B**) FLG, and (**C**) both IL-37 and FLG in healthy skin biopsies. ***(Continued)***

indicated DAPI nuclear staining, red indicated staining for IVL/FLG2/IL-37, and green indicated staining for FLG. The Pen tool was used to annotate the edge of the tissue. Based on the annotation, two margins indicated as inner and outer layers (50 micron) were set include most of the epidermis (Supplemental Fig. 2A–D). The first margin (outer) included stratum corneum and stratum granulosum, which were enriched for mature keratinocytes. The second margin (inner) included stratum spinosum and stratum basale, which contained mainly basal keratinocytes. After defining the margins for the epidermis, algorithms from Indica Labs were used to measure the expression of each marker, and the cytoplasmic and nuclear immunostaining was quantified (Area Quantification FL v2.1.1 and CytoNuclear FL v 1.4) (Supplemental Fig. 2E, 2F).

Statistics

All p values reported in this analysis are two-tailed. All comparisons between means of discrete groups were performed using the two-tailed unpaired Student t test. Student t test p values were determined in R using the t.test function, which follows standard procedures for determining significance. All correlation coefficients were Pearson correlation coefficients, except where noted. Pearson and Spearman correlation coefficients and p values were determined using the cor.test function in R, which follows the standard procedures. With this value, the t statistic and the p value were calculated from the Student t distribution with df $n - 2$. Spearman correlation coefficients are determined as the Pearson correlation values of the ranks of the data. To determine Spearman correlation p values, we determine the Pearson correlation of the ranks and then follow the same procedures noted above. For the immunohistochemical staining in healthy controls and AD patients, an asterisk (*) indicates significant difference between healthy controls and AD patients by two-way ANOVA with Fisher least significant difference (LSD) posttest. For quantitative RT-PCR, an asterisk (*) indicates significant compared between healthy tissues and AD tissues by unpaired t test.

RESULTS

IL-37 and EDCs expression in skin RNA sequencing datasets

Expression of *FLG* and *FLG2* mRNA and protein level are well associated with the development of AD in humans (9). Based on this observation, publicly available transcriptome datasets were analyzed to identify genes that are associated with the decrease in *FLG* and *FLG2* expression in AD patients. Genes encoding structural proteins accounted for the majority of the 50 genes most closely associated with attenuated *FLG* and *FLG2* in AD patient skin. Notably, *IL1F7*, which encodes the cytokine IL-37, was also significantly downregulated in AD patients compared with healthy controls (Fig. 1A). Transcripts for EDC genes including *FLG* and *FLG2* were also reduced in AD patient skin compared with healthy controls (Fig 1B, 1C). Expression of *FLG* and *FLG2* were both reduced (albeit to a lesser degree than *IL1F7*) in majority of the published datasets, with only two datasets (GSE60709 and GSE75890) showing no change in *FLG* and *FLG2* expression compared with controls.

To further examinate the decrease of *IL-37* and EDCs in AD patients, we then performed analysis using data that were collected in previous clinical trial. This allowed us to further examine and correlate *IL-37* with EDC expression in AD patients by comparing lesional and nonlesional samples (Fig. 2). For the expression of *IL-37*, *FLG*, and *FLG2*, we observed a significant decrease of *IL-37* mRNA in lesional AD skin sample (dark blue) compared with nonlesional AD skin samples (light blue) (Fig. 2A). Interestingly, we did not observe any statistically difference between lesional and nonlesional AD skin samples for the expression of *FLG* and *FLG2* (Fig. 2B, 2C). We also perform correlation analysis to better understand the potential role of IL-37 in AD patient's skin. We observed a high correlation between IL-37 with FLG2 (correlation coefficient = 0.698) and FLG (correlation coefficient = 0.481) (Fig. 2D). The overlay histogram depicted the drastic decrease of *IL-37* expression in lesional AD skin samples (light blue) to the nonlesional AD skin samples (dark blue) (Fig. 2D).

It has been previously reported that there are five *IL1F7* transcript variants encoding different IL-37 isoforms (18). To understand the expression of these variant isoforms in AD patients, we performed analysis on publicly available RNA sequencing datasets to examine the distribution and expression of *IL1F7* transcript variants in AD patients. Isoform b (NM_014439.3) was the most abundant *IL1F7* transcript in healthy human skin (Supplemental Fig. 1A), in agreement with literature showing *IL1F7b* that is the effective and dominant transcript in the skin (23). Surprisingly, isoform e (NM_173204.1) was also highly expressed in healthy skin, a finding that has not been previously reported (Supplemental Fig. 1A). In AD skin samples, we observed

(**D**) Cell number for the epidermis in healthy controls (black), AD-1 trial (blue), and AD-2 trial (red). (**E**) DAPI staining within the outer and inner layers of epidermis. Immunofluorescent staining of IL-37 in (**F**) healthy control and patients from (**G**) AD-1 and (**H**) AD-2 trials. (**I**) Overall expression of IL-37 in five healthy controls and 10 patients from both AD-1 and AD-2 trials. Immunofluorescent staining of FLG in (**J**) healthy control and patients from (**K**) AD-1 and (**L**) AD-2 trials. (**M**) Overall expression of FLG in all three cohorts. (**N**) IL-37 and (**O**) FLG intensity in healthy controls ($n = 5$) and AD patients from two trials (AD-1 and AD-2) ($n = 10$ per trial). *$p < 0.05$ for healthy controls to AD patients, **$p < 0.01$ for healthy controls to AD patients, ***$p < 0.001$ for healthy controls to AD patients, ****$p < 0.0001$ for healthy controls to AD patients by two-way ANOVA with Fisher LSD posttest.

https://doi.org/10.4049/immunohorizons.2100055

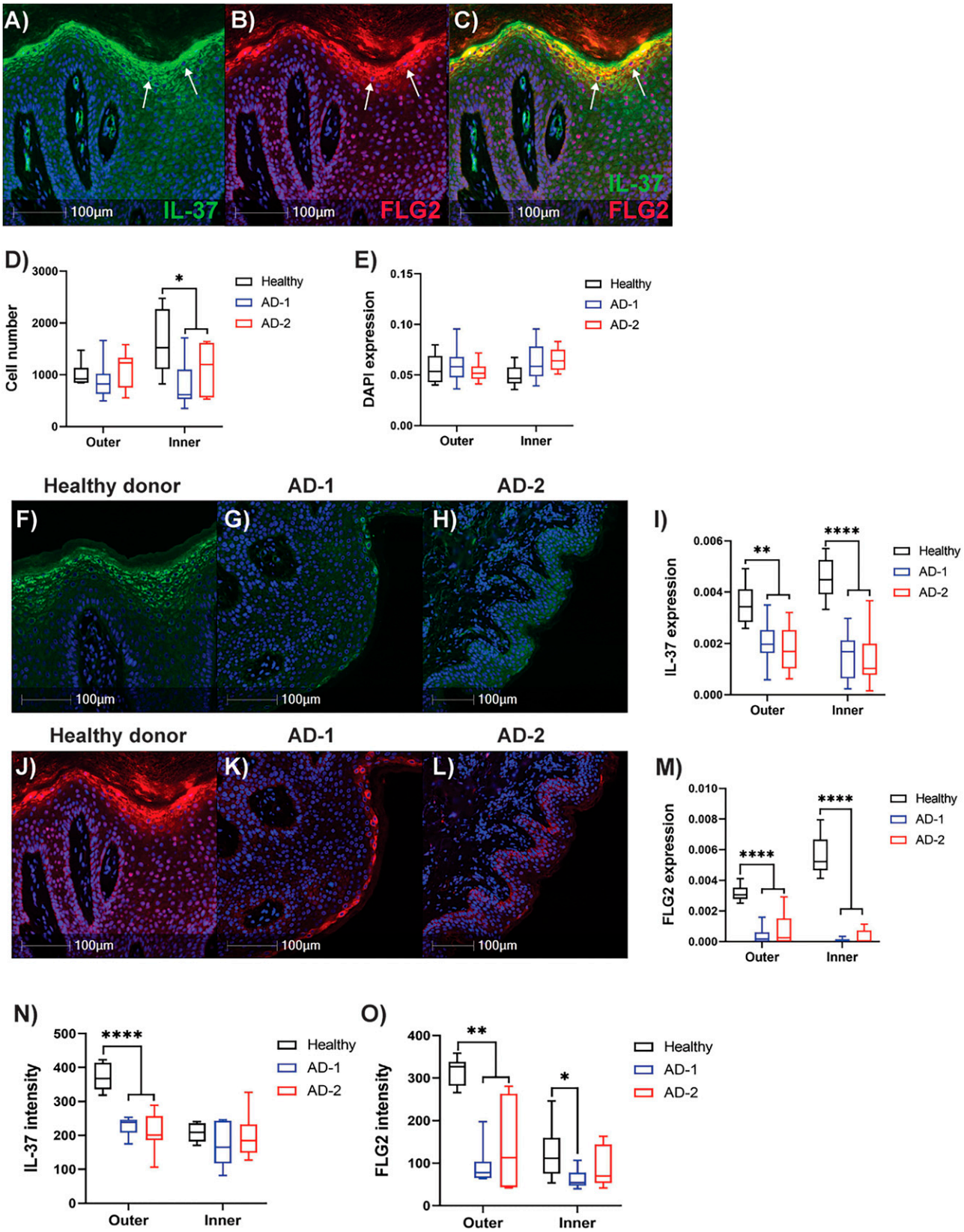

FIGURE 4. Immunofluorescent staining of FLG2 and IL-37 in healthy and AD skin biopsies.

Immunostaining against (**A**) IL-37 (green), (**B**) FLG2 (red), and (**C**) both IL-37 and FLG2 in healthy skin biopsies. The nuclear staining (DAPI) is in blue. (**D**) Cell number for the epidermis in healthy controls (black), AD-1 trial (blue), and AD-2 trial (red). (**E**) DAPI staining within the outer ***(Continued)***

that the expression of all *IL-37* isoforms was similar to that in nonlesional AD skin samples compared with healthy skin (Supplemental Fig. 1A). In contrast, there was a 2-fold reduction in *IL-37* transcript isoforms in lesional AD skin samples. Most noticeable were reductions in *IL-37b* and *IL-37d* (NM_173203.1) (Supplemental Fig. 1A). To further investigate these findings, *IL1F7* transcript variants were analyzed in laser capture microdissected nonlesional, acute lesional, and chronic lesional AD skin specimens. Isoform b was the most highly expressed isoform in the epidermal fraction of nonlesional AD skin and was the isoform most notably reduced in epidermal fractions from acute and chronic AD skin lesion (Supplemental Fig. 1B).

IHC of IL-37 and FLG, FLG2, and IVL in AD and healthy skin samples

To extend the aforementioned observations to the protein level, immunofluorescence was used to evaluate IL-37, FLG, FLG2, and IVL staining in AD skin biopsy specimens collected from clinical trials (AD-1 and AD-2) versus commercially sourced healthy control skin. Staining for IL-37 was predominately localized to the outermost layers of the epidermis (Fig. 3A). A similar staining pattern was seen with FLG (Fig. 3B). Isotype control (IgG) was included in all samples, and negligible background staining was observed. In overlaid images of IL-37 and FLG staining, there was a high degree of colocalization for these proteins, indicated by white arrow (Fig. 3C). We observed a decrease of total cell number in the inner layer of the skin in both set of AD samples; however, there was no change in the nuclear staining in either outer layer of the skin, but we did observe statistically difference in the inner skin layer for AD patients in AD-1 cohort. (Fig. 3D, 3E). Expression of IL-37 was also decreased in AD skin specimens, with only a few cells expressing IL-37 in the uppermost layers of the epidermis (Fig. 3F–I). FLG was significantly reduced in the epidermis of AD samples versus healthy skin specimens (Fig. 4J–M). The concomitant reduction in FLG and IL-37 in AD lesional skin was seen in representative samples (AD-1 and AD-2) from two separate clinical trials (Fig. 4N, 4O).

We confirmed the same coregulated pattern of IL-37 expression in relation to FLG2 (Fig. 4A, 4B). The localization of FLG2 in healthy human skin was similar to that seen with FLG. Colocalization of IL-37 with FLG2 in healthy human skin was also similar to that seen for FLG (Fig. 4C). We observed a decrease of cell number in the inner skin layer in both AD cohorts (AD-1 and AD-2) compared with healthy controls (Fig. 4D). However, we did not observe any difference between healthy control to AD patients in the DAPI expression (Fig. 4E). Similar to FLG (Fig. 3), FLG2 protein expression (and IL-37) was reduced in AD skin specimens compared with healthy skin biopsies (Fig. 4F–M), as was the overall intensity of FLG2 and IL-37 in all AD samples (Fig. 4N, 4O).

The distribution of IVL staining was more widespread in the epidermis compared with FLG (Fig. 3), FLG2 (Fig. 4), and IL-37 (Fig. 5A, 5B). In overlaid images, IL-37 colocalized with IVL in the outer layers of the epidermis but not with IVL signal lower in the stratum spinosum (Fig. 5C). In AD skin, IVL protein was significantly reduced compared with healthy skin biopsies (Fig. 5F–O). Interestingly, the overall intensity of IVL was significantly decreased in the inner layer in both AD trails compared with healthy control skin (Fig. 5O). This could also be seen on the IHC staining (Fig. 5J, 5L). In addition to immunofluorescence studies with skin, ELISA analysis of serum samples from the same donors was performed to measure circulating IL-37 levels. However, IL-37 was not detectable in either set of AD patients or healthy control samples (data not shown).

IHC of IL-37 and FLG, FLG2, and IVL in human 3D full thickness skin model (EpidermFT)

Transcriptomic analysis was conducted in the EpidermFT in vitro human 3D full thickness skin model to characterize the potential to use this system to understand the role of IL-37 in normal skin biology and AD pathogenesis. Adding the T_h2 cytokines IL-4, IL-13, and IL-31 to this system can be used to model an AD skin phenotype (Fig. 6A–D) (22). Using the combination of all three cytokines in this model, we observed the structural changes in the epidermis that mimic AD in humans. In addition, this provided a tractable system to understand IL-37 protein localization and regulation in the skin. Interestingly, transcript levels of total *IL-37* were also reduced in this AD-like tissue (EpidermFT-400 3D with Atopic Dermatitis [EpidermFT-AD]). The reduction in *IL-37* in the EpidermFT-AD model was more profound when compared with that observed in human AD skin specimens, Similar to studies with human specimens, *IL1F7*, *FLG*, and *FLG2* levels correlated with one another in the EpidermFT model (Fig. 6E, 6F). The transcriptomic study–based observations were also validated with quantitative PCR, showing significantly reduced *IL1F7* and EDCs (*FLG*, *FLG2*, *LOR*, and *IVL)* transcripts in AD model (EpidermFT-AD) compared the healthy control model (EpidermFT) samples (Fig. 6G–K). At the protein level, immunofluorescence analysis revealed interesting information about the localization of IL-37 and EDC proteins in the 3D skin model. In this model, FLG, FLG2, and IVL and IL-37 all colocalized to the outer part of the epidermal layer. In the AD-like

and inner layers of epidermis. Immunofluorescent staining of IL-37 in (**F**) healthy control and patients from (**G**) AD-1 and (**H**) AD-2 trials. (**I**) Overall expression of IL-37 in healthy controls ($n = 5$), AD-1 ($n = 10$), and AD-2 ($n = 10$). Immunofluorescent staining of FLG2 in (**J**) healthy control and patients from (**K**) AD-1 and (**L**) AD-2 trials. (**M**) Overall expression of FLG in all three cohorts. (**N**) IL-37 and (**O**) FLG2 intensity in healthy controls ($n = 5$) and AD patients from two trials (AD-1 and AD-2) ($n = 10$ per trial). *$p < 0.05$ for healthy controls to AD patients, **$p < 0.01$ for healthy controls to AD patients, ****$p < 0.0001$ for healthy controls to AD patients by two-way ANOVA with Fisher LSD posttest.

https://doi.org/10.4049/immunohorizons.2100055

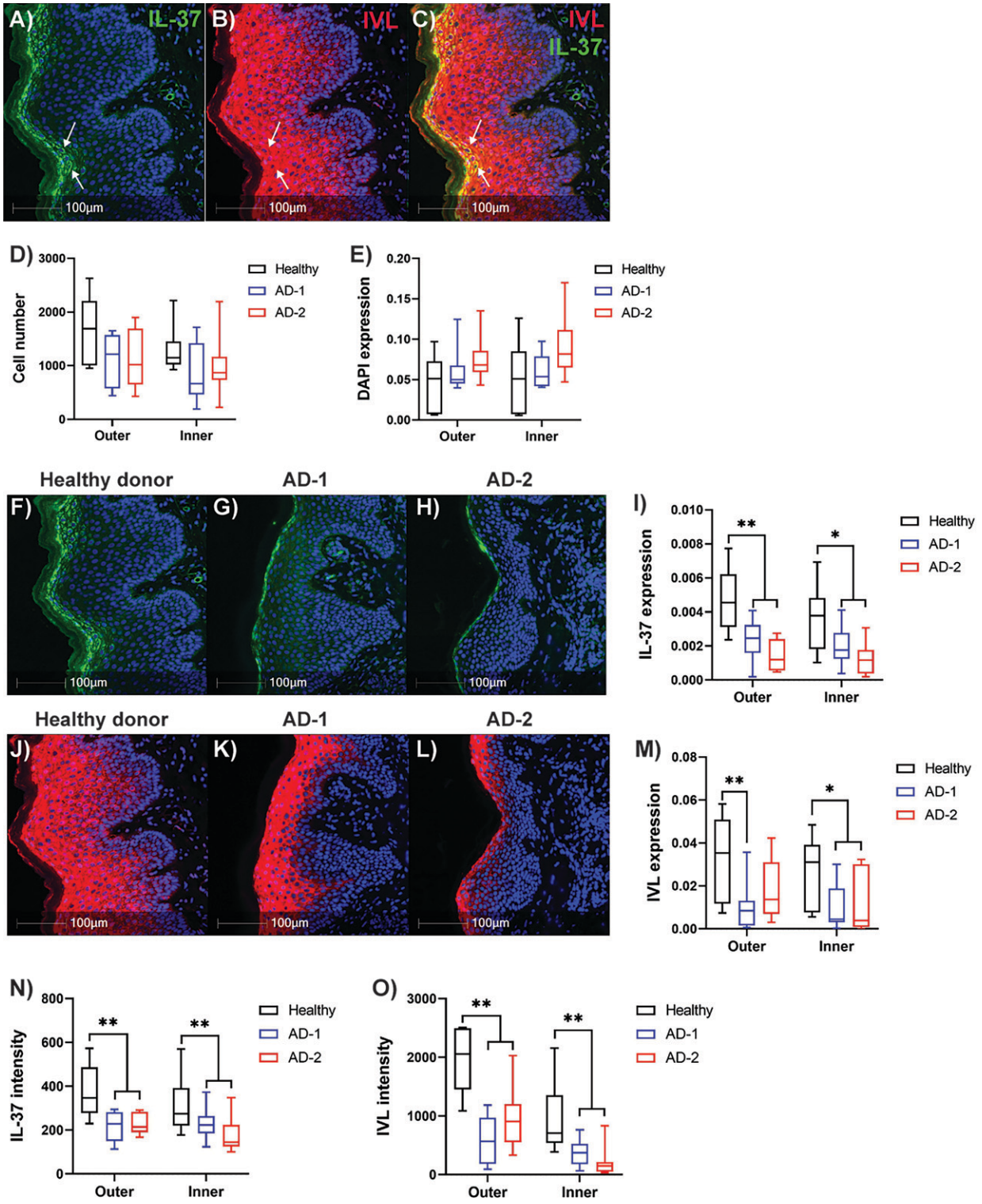

FIGURE 5. Immunofluorescent staining of IVL and IL-37 in healthy and AD skin biopsies.

Immunostaining against (**A**) IL-37 (green), (**B**) IVL (red) and (**C**) costaining of IL-37 and IVL in healthy skin biopsies. (**D**) Cell number in the epidermis in healthy controls (black), AD-1 trial (blue), and AD-2 trial (red). (**E**) DAPI staining within the outer and inner layers of epidermis. The nuclear staining (DAPI) is in blue. Immunofluorescent staining of IL-37 (green) in (**F**) healthy control and patients from (**G**) AD-1 and (**H**) AD-2 trials. (**I**) Overall expression of IL-37 in healthy controls ($n = 5$) and AD-1 ($n = 10$) and AD-2 ($n = 10$). Immunofluorescent staining of IVL (red) in (**J**) healthy control, (**K**) patient from AD-1 trial, and (**L**) patient from AD-2 trial. (**M**) Overall expression of IVL in all three cohorts. (**N**) IL-37 and (**O**) IVL intensity in healthy controls ($n = 5$) and AD patients from two trials (AD-1 and AD-2) ($n = 10$ per trial). *$p < 0.05$ for healthy controls to AD patients, **$p < 0.01$ for healthy controls to AD patients for healthy controls to AD patients by two-way ANOVA with Fisher LSD posttest.

https://doi.org/10.4049/immunohorizons.2100055

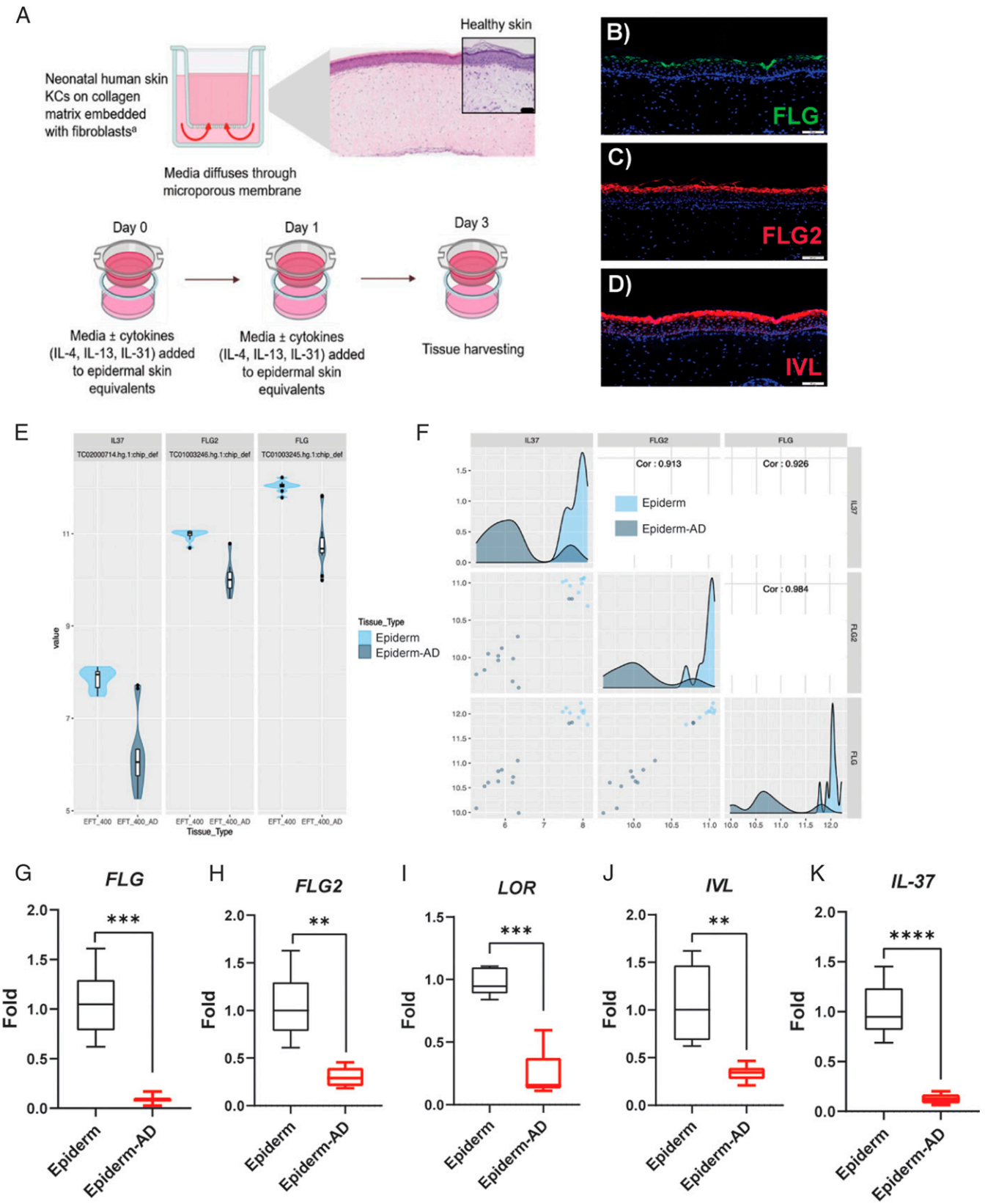

FIGURE 6. Gene expression and immunofluorescent staining in full thickness EpidermFT human skin model.

Human in vitro 3D skin model (EpidermFT) consists of neonatal derived human keratinocytes on a collagen matrix embedded on human fibroblasts. This model is a well-established in vitro skin model for validation. (**A**) Culture scheme for the human skin 3D model. rIL-4, IL-13, and ***(Continued)***

https://doi.org/10.4049/immunohorizons.2100055

specimens (EpidermFT-AD), expression FLG (Fig. 7A–C), FLG2 (Fig. 7D–E), IVL (Fig. 7G–I), and IL-37 (Fig. 7J–L) were all reduced compared with EpidermFT samples (i.e., nontreated IL-4, IL-13, and IL-31). These observations parallel those seen with healthy and AD human skin specimens and demonstrate the sufficiency of T_h2 cytokines to directly attenuate IL-37, FLG, FLG2, and IVL expression.

Effect of IL-37 in 3D human skin tissues

To better understand the role of IL-37 in skin biology, studies were performed to determine if exogenous IL-37 could alter EDC protein levels in the EpidermFT model system. Relative to untreated controls, adding increasing concentrations of IL-37 to the culture media led to increased FLG and FLG2 protein expression in the outer layer of the epidermis (Fig. 8A–F). No such effect was seen for IVL with IL-37 treatment (Fig. 8G–I).

DISCUSSION

AD is one of the most prevalent inflammatory diseases in developed countries. The recent development and approval of new medications, like dupilumab and baricitinib, have provided more treatment options for moderate-to-severe AD. However, there is still a large unmet need for therapeutics.

The current studies used transcriptomic analysis of publicly available datasets to show IL-37 transcript (*IL1F7*) expression is reduced in AD skin, especially in lesional specimens (Figs. 1, 2). The most prominent reduction in IL-37 were observed in chronic AD lesional skin. Interestingly, it has previously been demonstrated that IL-37 expression is also reduced in psoriatic skin specimens (24). Owing to its anti-inflammatory properties, reduced levels of IL-37 might impact the inflammatory milieu of the skin microenvironment. Thus, measures to restore IL-37 expression or activity in AD could be a novel means to treat this and perhaps other inflammatory skin diseases. In the current studies, we used meta-analysis of public and clinical trial data to understand the relationship of IL-37 with AD. Furthermore, we have shown that the IL-37 protein is expressed in the epidermis of healthy human skin and that the expression of IL-37 is decreased in AD patients.

In the meta-analysis using publicly available data and internal clinical trial materials, because of the variation in experimental planning and execution, all the data were collected and normalized, allowing for comparison across all datasets. Through this combinatorial assessment, we observed a decrease in IL-37 expression in AD skin biopsies compared with healthy skin biopsies (Figs. 1, 2). This observation indicated the potential role of IL-37 in skin and how the loss of *IL-37* correlated with AD disease progression. In the same analysis, we also verified the changes in skin EDCs, and we observed significant reduction in *FLG* and *FLG2* expression, three key structural EDCs in skin (Fig. 1). The reduce expression of these three transcripts/proteins has been reported previous in AD patients. We then analyzed the correlation between *IL-37* expression and EDCs in AD patients compared with healthy donors. We observed a positive correlation between the decrease in IL-37 expression with a decrease in *FLG*, *FLG2*, and *IVL* expression. This observation provided, to our knowledge, first insight into the possible relationship of IL-37 with skin structural EDCs.

After gaining insight in the transcriptional expression of IL-37 in both healthy and AD patient biopsies, we performed immunofluorescence to localize the expression of IL-37, first in healthy human skin. We demonstrated most of IL-37 protein expression exists in the outer layers of the epidermis. The magnified image showed diffusion of IL-37 protein past the stratum corneum (highlighted in red) in Figs. 4–6. Although this observation was in alignment with a previous observation by Lachner et al. (25), our finding, to our knowledge, was the first to illustrate an image format that characterizes the diffusion of IL-37 in epidermis. Based on our observation in the IHC staining of IL-37, it is strongly suggested that IL-37 production is performed in more mature or differentiated epidermal keratinocytes (Figs. 3–5). This observation is further supported by the high degree of costaining seen between IL-37 and both FLG and FLG2 compared with the partial overlap seen with IVL (Figs. 3–5). This colocalization raised the possibility that IL-37 could regulate EDC gene expression and skin barrier function.

Immunofluorescence staining revealed a spectrum of reduced to completely absent IL-37 expression in AD skin specimens. This finding paralleled with reductions in *IL1F7* transcripts (encoding IL-37). Immunofluorescence studies also demonstrated reductions in FLG, FLG2, and IVL in AD patient skin (Figs. 3–5). Interestingly, and in contrast to FLG and IVL, FLG2 staining was present from basal to stratum corneum layers of the epidermis. In AD patient, the loss of FLG2 was mainly observed in the stratum corneum; however, the FLG2 level at the basal layer was mostly retained. Overall, we observed a loss of IL-37, FLG, FLG2, and IVL in the epidermis in AD patients compared with healthy donors.

IL-31 are added in the culture media to create an AD tissue. This method has been documented in the poster presentation. Immunofluorescent staining of (**B**) FLG (green), (**C**) FLG2 (red), and (**D**) IVL (red) in healthy tissue (EpidermFT). The magnification for the image was 100×. The nuclear staining (DAPI) is in blue. (**E**) Meta-analysis of IL-37, FLG, FLG2, and IVL expression in healthy tissues (EpidermFT) and AD tissues (EpidermFT-AD). (**F**) Correlation of IL-37 expression with FLG, FLG2, and IVL. (**G**–**K**) Quantitative RT-PCR (qRT-PCR) analysis of healthy and AD tissues. Each group includes three independent experiments, with two tissues in each experiment. $^{**}p < 0.01$ for healthy tissues to AD tissues, $^{***}p < 0.001$ for healthy tissues to AD tissues, $^{****}p < 0.0001$ for healthy tissues to AD tissues by unpaired *t* test.

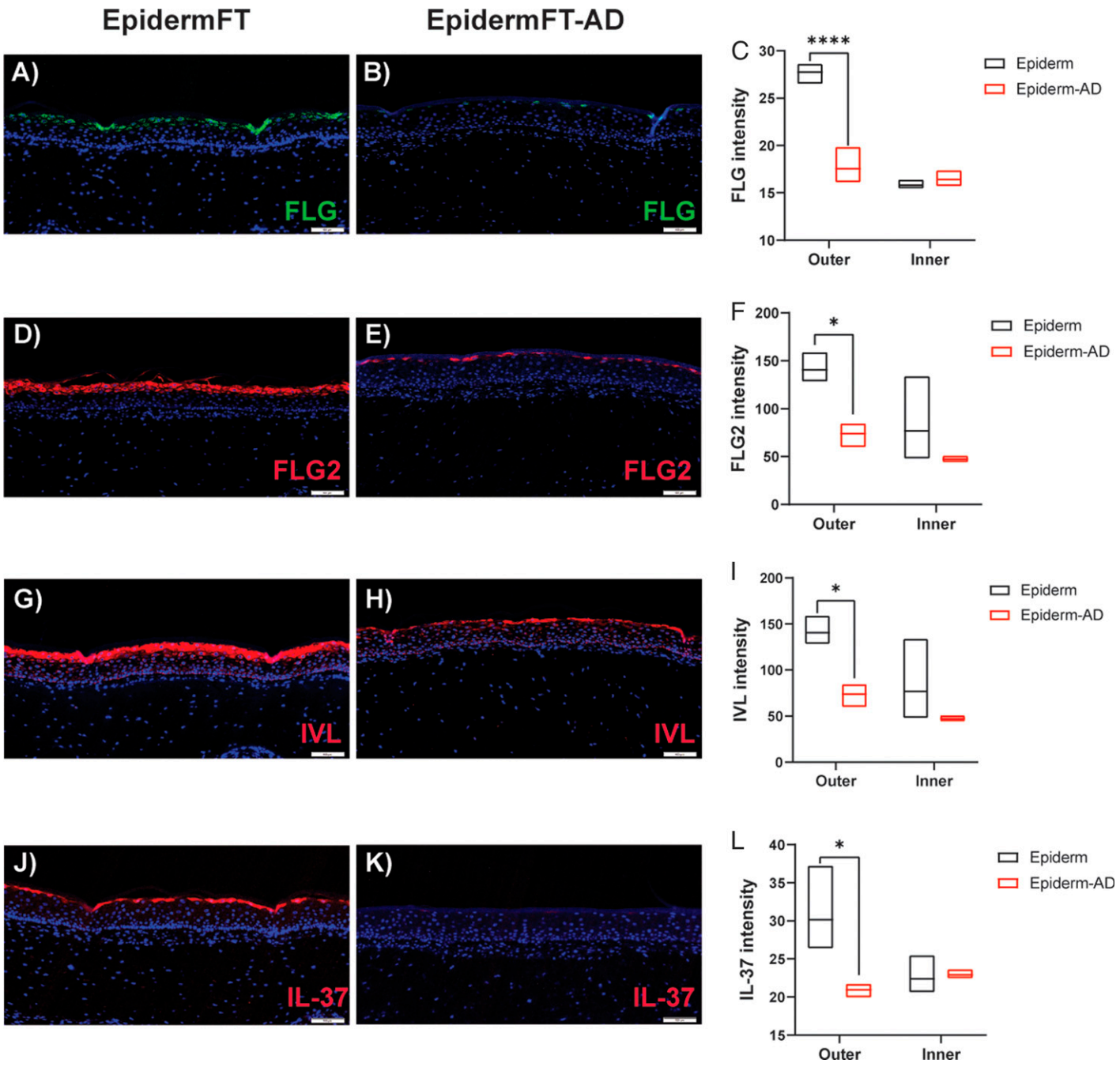

FIGURE 7. Immunofluorescent staining of FLG, FLG2, IVL, and IL-37 in EpidermFT model.

Immunofluorescent staining in healthy (EpidermFT) and AD (EpidermFT-AD) tissues. (**A** and **B**) FLG (green) staining in healthy and AD tissues. (**C**) Overall intensity of FLG in both tissues. (**D** and **E**) FLG2 (red) staining in healthy and AD tissues. (**F**) FLG2 intensity in healthy or AD tissues. (**G** and **H**) IVL (red) staining in healthy and AD tissues. (**I**) IVL intensity in both tissues. (**J** and **K**) IL-37 (red) staining in healthy and AD tissues. The nuclear staining (DAPI) is in blue. (**L**) Overall intensity of IL-37 in healthy or AD tissues. *$p < 0.05$ for healthy tissues to AD tissues, ****$p < 0.0001$ for healthy tissues to AD tissues by two-way ANOVA with Fisher LSD posttest.

In the EpidermFT in vitro 3D human skin model, T_h2 cytokines (IL-4, IL-13, and IL-31) were sufficient to reduce IL-37 and EDC gene and protein expression. This in vitro system has been used to model different skin diseases, including AD (22). Immunofluorescence staining in this model recapitulated important aspects of immunofluorescence staining in healthy and AD donor skin specimens. Similar to human skin, IL-37, FLG, FLG2, and IVL were most prominent in the upper epidermal layers in this model. However, expression of IL-37, FLG, FLG2, and IVL was less diffuse in this model compared with human skin (Fig. 6).

https://doi.org/10.4049/immunohorizons.2100055

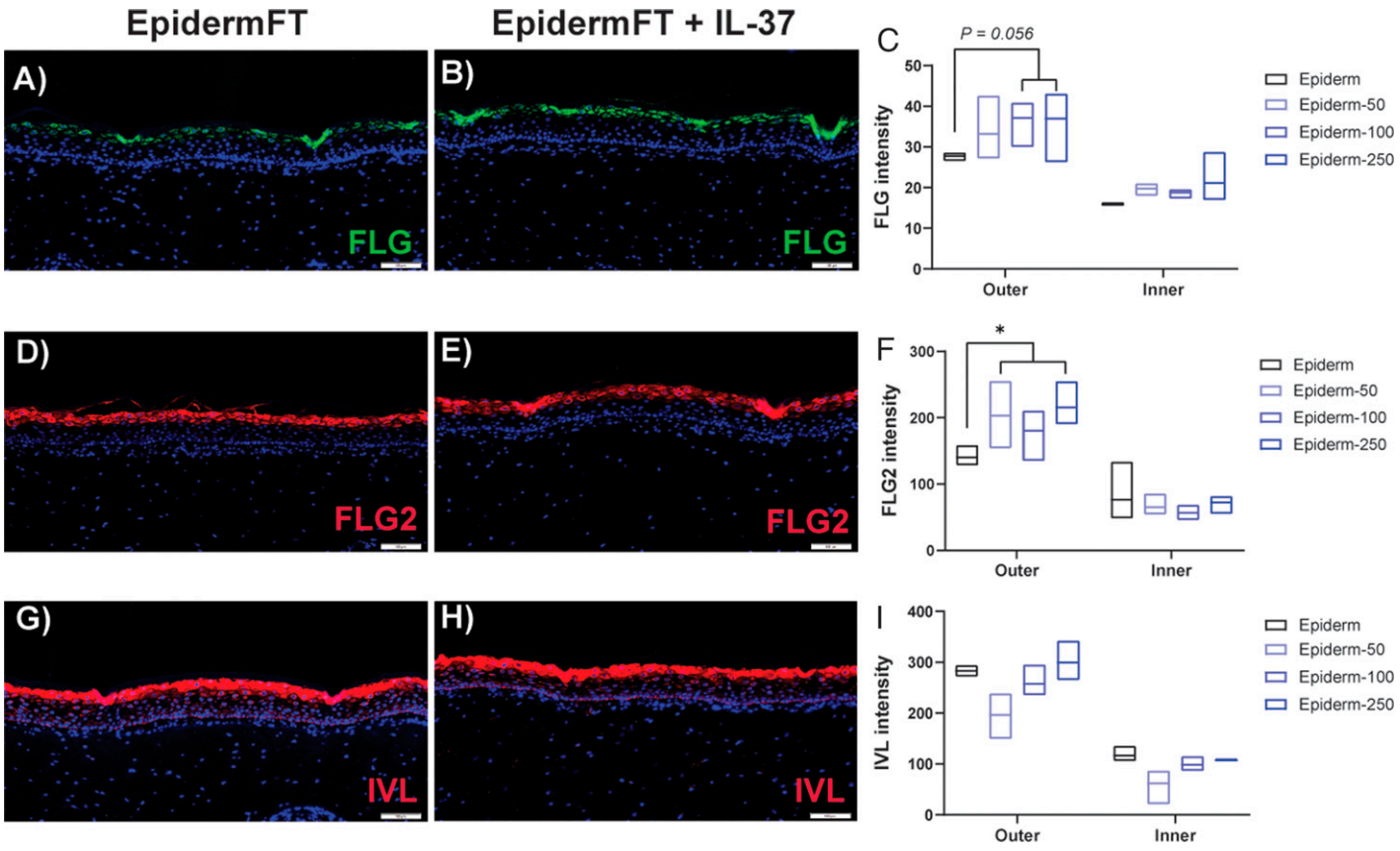

FIGURE 8. Effect of rhIL-37 in EpidermFT model.

Immunofluorescent staining of (**A** and **B**) FLG (green), (**D** and **E**) FLG2 (red), and (**G** and **H**) IVL (red) in healthy tissues (EpidermFT) or rhIL-37 (100 ng/ml)–treated tissues (EpidermFT + IL-37). The nuclear staining (DAPI) is in blue. (**C**) Overall intensity of FLG expression in healthy tissues or rhIL-37-treated (50, 100, and 250 ng/ml) tissues. The change of blue color indicates increase concentration of IL-37 in the media. (**F**) Overall intensity of FLG2 in healthy tissues or IL-37-treated (50, 100, and 250 ng/ml) tissues. (**I**) Overall intensity of IVL in healthy tissues or IL-37-treated (50, 100, and 250 ng/ml) tissues. *$p < 0.05$ for healthy tissues to AD tissues by two-way ANOVA with Fisher LSD posttest.

After confirming the expression and localization of IL-37 in the EpidermFT model, we studied the effects of exogenous human rIL-37 on skin EDC gene/protein expression. Compared with unstimulated control samples, stimulation of EpidermFT samples with rhIL-37 for 3 d increased FLG and FLG2 (Fig. 8). Interestingly, addition of IL-37 did not change the expression of IVL. It seems like IL-37 selectively affects FLG and FLG2, but not all the EDCs. Further experiments are needed to better understand how IL-37 affects skin EDCs in different capacity. In addition, this is, to our knowledge, the first report demonstrating IL-37 that can regulate EDC members. Further analysis on how IL-37 regulates EDC expression in this model is required.

The data presented in this study suggest the T_h2-polarized inflammatory milieu could attenuate IL-37 expression in AD skin lesions. In light of the ability of rIL-37 to reduce EDC expression in the EpidermFT model system, it is also conceivable that the reduction in IL-37 in AD patient skin could contribute to decreased expression of EDC proteins. The ability of IL-37 to directly impact EDC expression provides, to our knowledge, a new insight into the possible biological mechanisms by which this cytokine may contribute to normal skin physiology and AD pathogenesis. Although additional studies are needed, the potential of IL-37 to directly impact EDC member expression and thus skin barrier function suggests this cytokine could become a novel therapeutic target for patients with AD.

DISCLOSURES

J.Z., D.C.G., J.T.S., and K.R.S. are employees and may be shareholders of Eli Lilly and Company. J.O. and J.M. are employees of MatTek Corporation. M.J.T. has no financial conflicts of interest.

ACKNOWLEDGMENTS

We thank Jeff Hanson at Eli Lilly and Company for the assistance in HALO and IHC image analysis.

REFERENCES

1. Rønnstad, A. T. M., A. S. Halling-Overgaard, C. R. Hamann, L. Skov, A. Egeberg, and J. P. Thyssen. 2018. Association of atopic dermatitis with depression, anxiety, and suicidal ideation in children and adults: a systematic review and meta-analysis. *J. Am. Acad. Dermatol.* 79: 448–456.e30.
2. Chovatiya, R., and J. I. Silverberg. 2019. Pathophysiology of atopic dermatitis and psoriasis: implications for management in children. *Children (Basel)*. 6: 108.
3. Silverberg, J. I., J. M. Gelfand, D. J. Margolis, M. Boguniewicz, L. Fonacier, M. H. Grayson, E. L. Simpson, P. Y. Ong, and Z. C. Chiesa Fuxench. 2018. Patient burden and quality of life in atopic dermatitis in US adults: a population-based cross-sectional study. *Ann. Allergy Asthma Immunol.* 121: 340–347.
4. Simpson, E. L., E. Guttman-Yassky, D. J. Margolis, S. R. Feldman, A. Qureshi, T. Hata, V. Mastey, W. Wei, L. Eckert, J. Chao, et al. 2018. Association of inadequately controlled disease and disease severity with patient-reported disease burden in adults with atopic dermatitis. *JAMA Dermatol.* 154: 903–912.
5. Moreno, A. S., R. McPhee, L. K. Arruda, and M. D. Howell. 2016. Targeting the T helper 2 inflammatory axis in atopic dermatitis. *Int. Arch. Allergy Immunol.* 171: 71–80.
6. Novak, N., T. Bieber, and D. Y. M. Leung. 2003. Immune mechanisms leading to atopic dermatitis. *J. Allergy Clin. Immunol.* 112(6, Suppl): S128–S139.
7. Armengot-Carbo, M., Á. Hernández-Martín, and A. Torrelo. 2015. The role of filaggrin in the skin barrier and disease development. *Actas Dermosifiliogr.* 106: 86–95.
8. Rerknimitr, P., A. Otsuka, C. Nakashima, and K. Kabashima. 2017. The etiopathogenesis of atopic dermatitis: barrier disruption, immunological derangement, and pruritus. *Inflamm. Regen.* 37: 14.
9. Osawa, R., M. Akiyama, and H. Shimizu. 2011. Filaggrin gene defects and the risk of developing allergic disorders. *Allergol. Int.* 60: 1–9.
10. Kim, B. E., and D. Y. M. Leung. 2018. Significance of skin barrier dysfunction in atopic dermatitis. *Allergy Asthma Immunol. Res.* 10: 207–215.
11. Kim, B. E., D. Y. Leung, M. Boguniewicz, and M. D. Howell. 2008. Loricrin and involucrin expression is down-regulated by Th2 cytokines through STAT-6. *Clin. Immunol.* 126: 332–337.
12. Kim, B. E., M. D. Howell, E. Guttman-Yassky, P. M. Gilleaudeau, I. R. Cardinale, M. Boguniewicz, J. G. Krueger, and D. Y. M. Leung. 2011. TNF-α downregulates filaggrin and loricrin through c-Jun N-terminal kinase: role for TNF-α antagonists to improve skin barrier. [Published erratum appears in 2011 *J. Invest. Dermatol.* 131: 1388.] *J. Invest. Dermatol.* 131: 1272–1279.
13. Sandilands, A., C. Sutherland, A. D. Irvine, and W. H. McLean. 2009. Filaggrin in the frontline: role in skin barrier function and disease. *J. Cell Sci.* 122: 1285–1294.
14. Gao, P.-S., N. M. Rafaels, T. Hand, T. Murray, M. Boguniewicz, T. Hata, L. Schneider, J. M. Hanifin, R. L. Gallo, L. Gao, et al. 2009. Filaggrin mutations that confer risk of atopic dermatitis confer greater risk for eczema herpeticum. *J. Allergy Clin. Immunol.* 124: 507–513.E7.
15. Morar, N., W. O. C. M. Cookson, J. I. Harper, and M. F. Moffatt. 2007. Filaggrin mutations in children with severe atopic dermatitis. *J. Invest. Dermatol.* 127: 1667–1672.
16. Elias, M. S., H. A. Long, C. F. Newman, P. A. Wilson, A. West, P. J. McGill, K. C. Wu, M. J. Donaldson, and N. J. Reynolds. 2017. Proteomic analysis of filaggrin deficiency identifies molecular signatures characteristic of atopic eczema. *J. Allergy Clin. Immunol.* 140: 1299–1309.
17. Wang, L., Y. Quan, Y. Yue, X. Heng, and F. Che. 2018. Interleukin-37: a crucial cytokine with multiple roles in disease and potentially clinical therapy. *Oncol. Lett.* 15: 4711–4719.
18. Ellisdon, A. M., C. A. Nold-Petry, L. D'Andrea, S. X. Cho, J. C. Lao, I. Rudloff, D. Ngo, C. Y. Lo, T. P. Soares da Costa, M. A. Perugini, et al. 2017. Homodimerization attenuates the anti-inflammatory activity of interleukin-37. *Sci. Immunol.* 2: eaaj1548.
19. Wald, D., J. Qin, Z. Zhao, Y. Qian, M. Naramura, L. Tian, J. Towne, J. E. Sims, G. R. Stark, and X. Li. 2003. SIGIRR, a negative regulator of Toll-like receptor-interleukin 1 receptor signaling. *Nat. Immunol.* 4: 920–927.
20. Garlanda, C., H. J. Anders, and A. Mantovani. 2009. TIR8/SIGIRR: an IL-1R/TLR family member with regulatory functions in inflammation and T cell polarization. *Trends Immunol.* 30: 439–446.
21. Glickman, M. E., S. R. Rao, and M. R. Schultz. 2014. False discovery rate control is a recommended alternative to Bonferroni-type adjustments in health studies. *J. Clin. Epidemiol.* 67: 850–857.
22. Hayden, P. J., J. P. Petrali, G. Stolper, T. A. Hamilton, G. R. Jackson, Jr., P. W. Wertz, S. Ito, W. J. Smith, and M. Klausner. 2009. Microvesicating effects of sulfur mustard on an in vitro human skin model. *Toxicol. In Vitro.* 23: 1396–1405.
23. Pan, Y., X. Wen, D. Hao, Y. Wang, L. Wang, G. He, and X. Jiang. 2020. The role of IL-37 in skin and connective tissue diseases. *Biomed. Pharmacother.* 122: 109705.
24. Rønholt, K., A. L.-L. Nielsen, C. Johansen, C. Vestergaard, A. Fauerbye, R. López-Vales, C. A. Dinarello, and L. Iversen. 2020. IL-37 expression is downregulated in lesional psoriasis skin. *ImmunoHorizons.* 4: 754–761.
25. Lachner, J., V. Mlitz, E. Tschachler, and L. Eckhart. 2017. Epidermal cornification is preceded by the expression of a keratinocyte-specific set of pyroptosis-related genes. *Sci. Rep.* 7: 17446.

https://doi.org/10.4049/immunohorizons.2100055